DOI: 10.1002/cmdc.201300571

Facile Identification of Dual FLT3–Aurora A Inhibitors: A Computer-Guided Drug Design Approach

Yung Chang Hsu, Yi-Yu Ke, Hui-Yi Shiao,* Chieh-Chien Lee, Wen-Hsing Lin, Chun-Hwa Chen, Kuei-Jung Yen, John T.-A. Hsu, Chungming Chang, and Hsing-Pang Hsieh*[a]

Computer-guided drug design is a powerful tool for drug discovery. Herein we disclose the use of this approach for the discovery of dual FMS-like receptor tyrosine kinase-3 (FLT3)–Aurora A inhibitors against cancer. An Aurora hit compound was selected as a starting point, from which 288 virtual molecules were screened. Subsequently, some of these were synthesized and evaluated for their capacity to inhibit FLT3 and Aurora kinase A. To further enhance FLT3 inhibition, structure–activity relationship studies of the lead compound were conducted through a simplification strategy and bioisosteric replacement, followed by the use of computer-guided drug design to prioritize molecules bearing a variety of different terminal groups in terms of favorable binding energy. Selected compounds were then synthesized, and their bioactivity was evaluated. Of these, one novel inhibitor was found to exhibit excellent inhibition of FLT3 and Aurora kinase A and exert a dramatic antiproliferative effect on MOLM-13 and MV4-11 cells, with an IC_{50} value of 7 nM. Accordingly, it is considered a highly promising candidate for further development.

Introduction

Protein kinases are a class of very important catalysts which transfer phosphate groups from ATP to specific substrates, thereby regulating cellular differentiation, growth, and migration.[1] Abnormal protein kinase activity is associated with cellular abnormalities such as the uncontrolled and rapid growth exhibited by cancer cells, and therefore, specific kinases are attractive targets for new chemotherapies.[1] In 2001, imatinib (Novartis) became the first small molecule kinase inhibitor to be approved by the US Food and Drug Administration for the treatment of chronic myeloid leukemia;[2] to date, twenty-five kinase inhibitors have been approved for the treatment of various cancers.[3,4]

Human protein kinases are classified into seven major groups by their sequence similarity and biochemical function.[5] Amongst the more than 500 kinases that have been identified, FMS-like receptor tyrosine kinase-3 (FLT3), a member of the class III tyrosine kinase receptor family, is expressed by immature hematopoietic cells and is strongly associated with acute myeloid leukemia (AML).[6] Overexpression of wild-type FLT3 often occurs in AML patients, and two major classes of activating FLT3 mutations (FLT3/ITD and FLT3/TKD) have been reported in approximately 30% of AML patients.[7,8] However, FLT3 inhibition as an AML treatment showed limited response in clinical studies, although it was proven as a critical factor for causing apoptosis in leukemia cells;[9–11] therefore, development of a highly efficient and low toxicity therapy has become an utmost priority.

Aurora kinases A, B, and C are members of the serine/threonine kinase family, which plays a critical role in cell mitosis.[12] In recent years, Aurora kinase has emerged as a potential molecular target in studies of solid tumors[12,13] and leukemia.[14] Notably, several studies demonstrated that dual FLT3–Aurora inhibition not only benefits patients with mutated FLT3 AML but is also effective against tumors that have acquired resistance to FLT3-selective inhibitors, due to the additional inhibition of Aurora kinase.[14,15] Therefore, dual FLT3–Aurora inhibitors may constitute an exciting new generation of treatments for AML.

The side chains of kinase inhibitors (though not the core) have been shown to play a critical role in kinase selectivity. For example, tandutinib (**1**),[16] AZD-1152HQPA (**2**),[17] gefitinib (**3**),[18] and lapatinib (**4**)[19] share the same quinazoline scaffold, which can form key interactions with the hinge region of kinases, and yet they target different kinases with varying degrees of selectivity (Figure 1). Similar results were observed by us: our recently discovered kinase inhibitors **5**[20] and **6**[21] share a common furanopyrimidine core, which forms hydrogen bonds with the hinge region of a protein kinase. However, **5**, bearing a urea side chain, was identified as an Aurora kinase A inhibitor, whereas **6**, with a chiral side chain, was found to be a selective EGFR inhibitor. This success encouraged the development of dual FLT3–Aurora A inhibitors, which focused on exploring the side chain moieties of 5,6-fused pyrimidine cores. Herein, the aim of this work was first to identify a potential dual FLT3–Aurora A inhibitor by using computer-guided drug

[a] Dr. Y. Chang Hsu, Dr. Y.-Y. Ke, Dr. H.-Y. Shiao, Dr. C.-C. Lee, Dr. W.-H. Lin, C.-H. Chen, K.-J. Yen, Dr. J. T.-A. Hsu, Dr. C. Chang, Dr. H.-P. Hsieh
Institute of Biotechnology & Pharmaceutical Research
National Health Research Institutes
35 Keyan Road, Zhunan, Miaoli County 350, Taiwan (ROC)
E-mail: hyshiao@nhri.org.tw
hphsieh@nhri.org.tw

Supporting information for this article is available on the WWW under http://dx.doi.org/10.1002/cmdc.201300571.

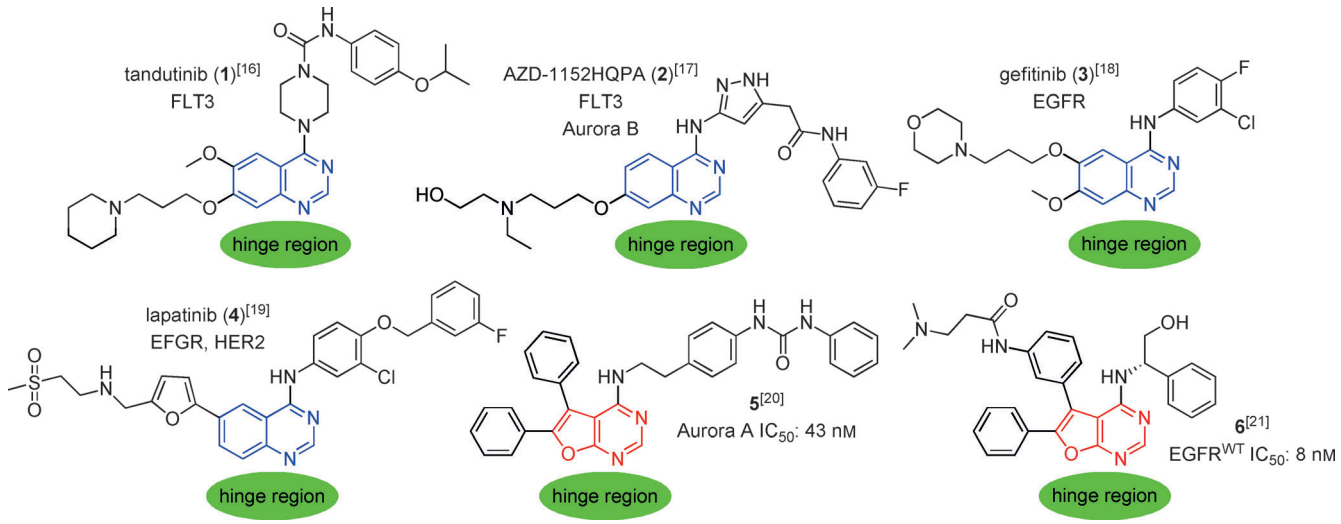

Figure 1. The quinazoline scaffold (blue) and the furanopyrimidine scaffold (red) form key hydrogen bonds to the kinase hinge region. By attaching different side chains, inhibitors can target distinct kinases with varying degrees of selectivity.

design to screen potential side chains using our newly built FLT3 model,[22] based on initial hit **5**, which was previously identified by high-throughput parallel synthesis technology and structure-based drug design.[20] Furthermore, dual inhibitor **27** was further improved in terms of both Aurora and FLT3 potency to obtain novel dual inhibitor **39** by bioisosterism and ring variations.

Results and Discussion

Identification of compound 27 from initial screening

As described in Scheme 1, using initial hit **5** as a starting point, a set of virtual molecules was designed and filtered in silico. A small selection of these was then synthesized, and their bioactivity was evaluated. Advantages of this strategy over the traditional synthetic medicinal chemistry approach include decreased effort and time in synthesis, as well as improved cost-effectiveness.

At first, the diphenylfuranopyrimidine skeleton of Aurora inhibitor **5** was adopted as the initial core, which was identified as crucial from our recent discovery.[20,21,23,24] We then collected 288 fragments (either commercially available or obtained from our previous kinase projects) as sources of side chain moieties. All of the identified fragments possessed common structural features, including a primary or secondary amino group, which could further act as the anchor to connect to the core. A virtual library of potential inhibitors (the diphenylfuranopyrimidine skeleton combined with each of the 288 fragments) was created in silico. Next, the FLT3 homology model established within our group[22] was introduced to the docking study with the docking score (103.154) of PHA739358 (moderate FLT3 inhibition, IC_{50} value of 669 nM)[25] as the minimal threshold (Table S1 and S2, Supporting Information). To gain structural diversity and minimize synthetic effort, we classified 154 molecules with higher score into

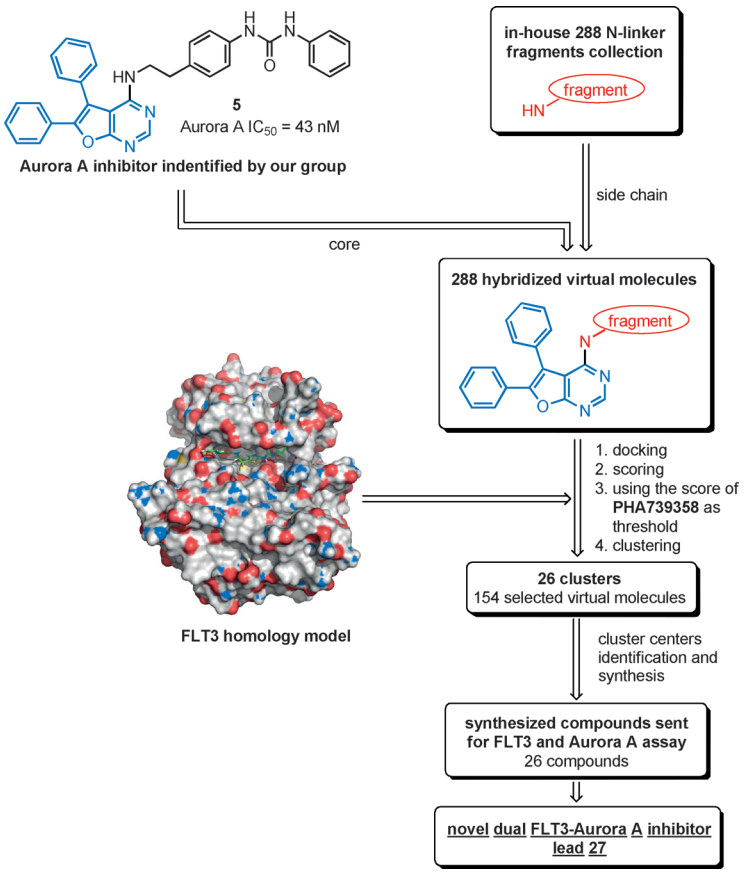

Scheme 1. Flowchart depicting the computer-guided strategy used to identify the dual FLT3–Aurora A inhibitor as our initial lead.

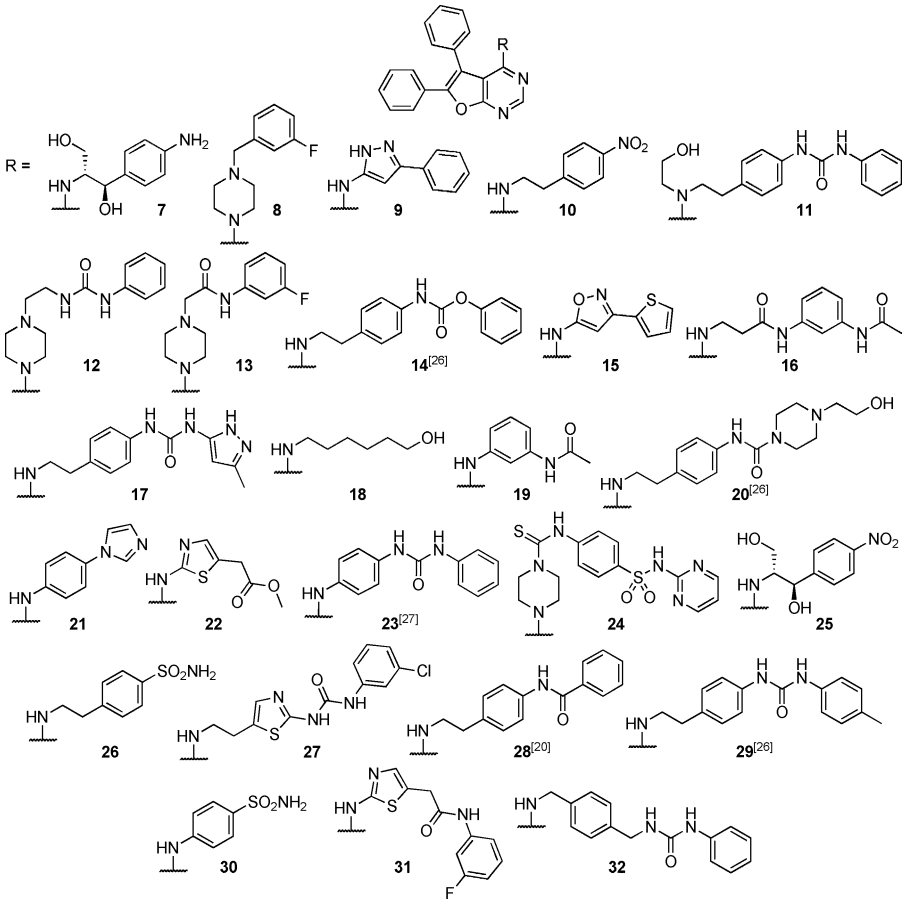

Scheme 2. Chemical structures of compounds **7**–**32**.

26 groups by the DS2.1/Cluster Ligands module. Thus, 26 molecules representing each group were selected for synthesis and subjected to in vitro enzyme-based testing of FLT3 and Aurora kinase A.

Chemical structures of all 26 synthesized molecules depicted in Scheme 2 and their inhibitory activities at 1.0 μM concentration against FLT3 and Aurora kinase A are listed in Table 1. Of these, more than half were found to inhibit Aurora kinase A by >50%. However, only compound **27** (cluster 21) imparted >30% inhibition of both kinases (59.0% inhibition of FLT3; 115.9% inhibition of Aurora kinase A) with IC_{50} values of 322 and 43 nM against FLT3 and Aurora kinase A, respectively (Table 2). Accordingly, **27** was selected for further optimization.

With **27** in hand, attempts were made to investigate structure–activity relationships. In our previous report,[27] the importance of phenyl rings (attached to the furanopyrimidine ring) for Aurora A inhibition was studied through a simplification strategy, and we found that the presence of a phenyl ring at the 6-position led to retention of activity. We thus introduced the same strategy in hopes of maintaining FLT3 potency while decreasing the molecular weight of **27** (M_r = 567 Da) to achieve a decrease in the clog*P* value. Furthermore, the oxygen atom of the furan does not appear to contribute a significant interaction within the hinge region, based on the docking study of **27**. Thus, removal of the furan phenyl ring, followed by bioisosteric replacement of the furan with a pyrrole, yielded compounds **33**–**36** (**33**, 6-phenyl furanopyrimidine; **34**, 5-phenyl furanopyrimidine; **35**, 6-phenyl pyrrolopyrimidine; **36**, 5-phenyl pyrrolopyrimidine). Subsequent FLT3/Aurora kinase A inhibitory assays were performed, with results shown in Table 2. Compounds **33**–**36** possessed similar Aurora A enzyme inhibition to that of lead compound **27**, suggesting that the position of the phenyl group was not important for Aurora kinase A activity. However, the presence of the phenyl group at the 6-position (but not at position 5) was found to be critical for FLT3 inhibition (IC_{50} value of 345 nM of **33**, compared with 780 nM for **34**; a similar trend was shown for **35** and **36**). More interestingly, compounds **35** and **36** showed a three- to sixfold improvement of FLT3 inhibition compared with **33** and **34**, indicating that the pyrrole moiety was more appropriate than furan within the hinge region of FLT3. Docking studies of **33** and **35** in the FLT3 homology model showed common hydrogen bonding between pyrimidine N1 and the kinase hinge region in a superpositioned conformation, while additional hydrogen bonding between the NH of the pyrrole ring and the carbonyl group of the Cys 694 backbone resulted in enhanced inhibition (**35**; Figure 2). In addition, compound **37** (with no substituents on the terminal phenyl moiety) was synthesized to verify the role of chlorine. The IC_{50} data for **37** showed that FLT3 inhibition was not significantly improved over that of **35**; however, Aurora kinase A inhibition increased threefold, suggesting that removal of the chlorine was essential. To further verify the predictive ability of our computer simulations, binding energy calculations were also carried out and showed direct correlation with the FLT3 IC_{50} values, as shown in Table 2. Therefore, binding energy calculations using our homology model were validated as a reliable strategy and used to guide our predictions of FLT3 activity of molecules in the next step.

Sequential screening for dual FLT3–Aurora A inhibitors

We next attempted to replace the phenyl group of the terminal side chain of **37** with a variety of heterocyclic groups using the above-mentioned computer-guided drug design. A set of 21 molecules were designed, based on bioisosteric utility and synthetic convenience, and their binding energies were calcu-

Table 1. Inhibition of FLT3 and Aurora kinase A (AKA) by compounds **7**–**32**.

Cluster	Representative Compd	Inhibition [%][a] FLT3	AKA
1	**7**	6.8	28.3
2	**8**	1.9	3.6
3	**9**	12.5	91.2
4	**10**	4.8	44.9
5	**11**	8.1	9.1
6	**12**	7.1	43.3
7	**13**	2.8	70.8
8	**14**[26]	6.5	96.3
9	**15**	3.8	7.0
10	**16**	11.3	84.0
11	**17**	3.1	97.3
12	**18**	4.6	85.8
13	**19**	17.6	72.9
14	**20**[26]	12.3	81.1
15	**21**	0.3	4.8
16	**22**	13.0	35.7
17	**23**[27]	13.8	28.3
18	**24**	18.3	16.7
19	**25**	3.0	5.5
20	**26**	10.6	80.1
21	**27**	59.0	115.9
22	**28**[20]	3.7	110.8
23	**29**[26]	0.6	95.5
24	**30**	6.5	53.7
25	**31**	20.4	6.4
26	**32**	4.1	70.1

[a] Inhibition was determined at a compound concentration of 1.0 μM. Data are representative values of single experiment determination (duplicate).

Table 2. Calculated binding energies (E_{bind}) for FLT3 and inhibitory activities of compounds **27** and **33**–**37** against FLT3 and Aurora kinase A (AKA).

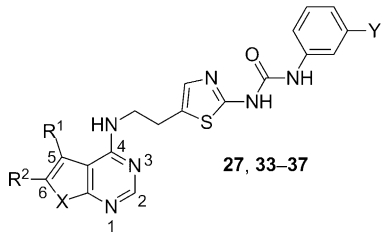

27, **33**–**37**

Compd	R^1	R^2	X	Y	E_{bind} [kcal mol^{-1}]	IC_{50} [nM][a] FLT3	AKA
27	Ph	Ph	O	Cl	−20.96	322 ± 30	43 ± 10
33	H	Ph	O	Cl	−20.99	345 ± 33	53 ± 2
34	Ph	H	O	Cl	−14.14	780 ± 108	80 ± 19
35	H	Ph	NH	Cl	−24.33	101 ± 11	32 ± 3
36	Ph	H	NH	Cl	−22.33	122 ± 10	42 ± 2
37	H	Ph	NH	H	−24.95	99 ± 17	9 ± 4

[a] Values represent the mean ± SD of at least two independent experiments performed in duplicate.

lated (Table S3, Supporting Information). Of these molecules, isoxazol-3-yl **38** was calculated to exhibit the lowest binding energy (−26.61 kcal mol^{-1}). To understand differences in binding conformations, **37** and **38** were analyzed within the FLT3 modeling structure (Figure 3). Similar binding was observed

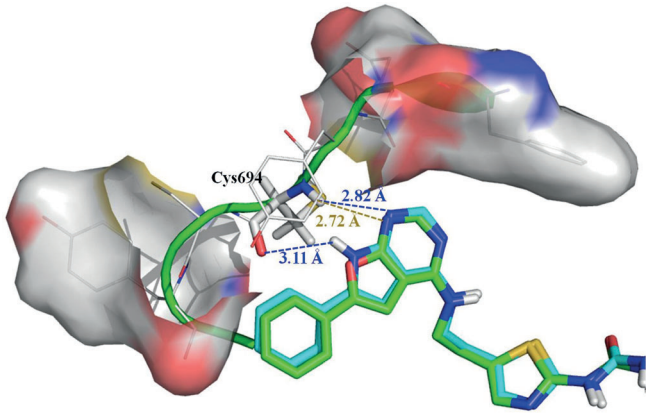

Figure 2. Docking studies of **33** (green) and **35** (blue) in the hinge region of the active site of the FLT3 homology model. Hydrogen bonding interactions between the protein and the ligand are shown as dotted lines. A common hydrogen bond was formed (shown on the figure) between the pyrimidine N1 and the kinase hinge region in a superposition of the binding conformation of two inhibitors. The NH in the pyrrole ring formed an additional hydrogen bond with the carbonyl group of the Cys694 backbone.

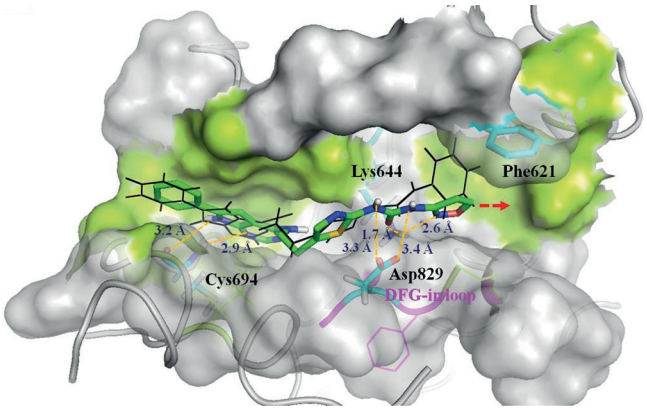

Figure 3. Docking studies of **37** (black) and **38** (green) in the active site of the FLT3 homology model. Hydrogen bonding interactions between the protein and the ligand are shown as yellow dotted lines. The terminal heterocyclic urea group of inhibitor **38** binds to FLT3 kinase, using four hydrogen bonds to Lys644 and Asp829, resulting in a different binding conformation of **38** compared with that of **37** and a lower binding energy. The extended functional group at the C5 position of the isoxazole moiety points toward the unoccupied hydrophobic region (red arrow), and may provide the accessory CH–π interaction with the phenyl group of the Phe621 residue.

between the pyrrolopyrimidine scaffold and the Cys694 backbone, but the position of the urea side chain of **38** was distinctly different from that of **37**: the nitrogen atom of the isoxazole and the oxygen atom of the urea from compound **38** formed two critical hydrogen bonds with Lys644. This resulted in the tail part of the side chain being pulled toward the DFG loop, such that two additional NH groups from the urea moiety could interact with Asp829. Furthermore, an unoccupied hydrophobic pocket near the Phe621 residue was observed, extending a suitable functional group at the C5-position of the isoxazole for a CH–π interaction with the phenyl group of phenylalanine. Based on an estimation of the distance between the extended group and Phe621, as well as the

rigidity of the modifying moiety, it was concluded that a *tert*-butyl group would be best suited to make this interaction.

Compounds **38** (isoxazol-3-yl moiety) and **39** (5-(*tert*-butyl)-isoxazol-3-yl moiety) were synthesized, and their enzymatic activity was evaluated (Table 3). They were found to impart slightly improved FLT3 inhibition and similar Aurora kinase A inhibition relative to **37**. In vitro testing of **38**, **39** (most promising in terms of enzymatic activities), and **5** (control) was used to evaluate their cellular activities in two acute monocytic leukemia (AML) cell lines (MOLM-13 and MV4-11). Compound **5** (with potent Aurora kinase A inhibition and no FLT3 inhibition) caused sub-micromolar antiproliferation, while compound **38** displayed approximately 7- and 10-fold improvement in antiproliferative activity in MOLM-13 and MV4-11, respectively. Compound **39** was found to be a much more potent inhibitor of both cell lines ($IC_{50} = 7$ nM), an unexpected result given its similar anti-kinase activity to **38**. This is probably due to the improved cellular permeability that results from the adjusted log *P* with the added the *tert*-butyl group.

Table 3. Calculated lipophilicity (clog *P*) of compounds **5**, **38**, and **39** and their inhibition of FLT3 and Aurora kinase A (AKA) as well as the MOLM-13 and MV4-11 cell lines.

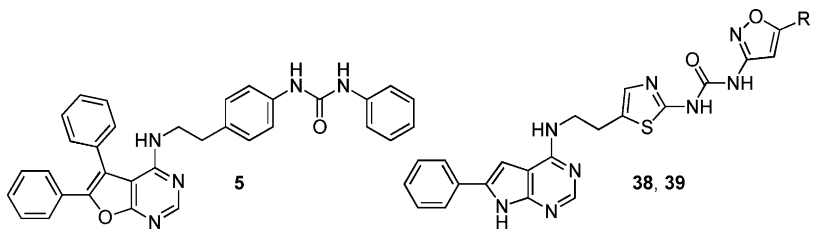

Compd	R	IC_{50} [nM][a]				clog *P*[b]
		FLT3	AKA	MOLM-13	MV4-11	
5[20]	–	>10000	57±12	481±88	654±63	5.62
38	H	77±6	13±0.3	65±9	68±8	1.2
39	*t*Bu	67±10	15±0.04	7±2	7±3	2.61

[a] Values represent the mean ±SD of at least two independent experiments performed in duplicate for enzyme-based assays and triplicate for cell-based assays. [b] Values were calculated using the Structure Design Suite from Advanced Chemistry Development, Inc. (Toronto, ON, Canada).

Due to the high antiproliferative activity of **39**, further protein immunoblot analysis in MV4-11 cells was conducted. Consistent with the enzyme-based assays, **39** displayed biomarker inhibition of phospho-FLT3 (Tyr591) and phospho-Aurora kinase A (Thr288) formation with an IC_{50} value of less than 50 nM (Figure 4), suggesting that the apoptosis of MV4-11 cells was caused by **39** through both FLT3 and Aurora kinase A inhibition.

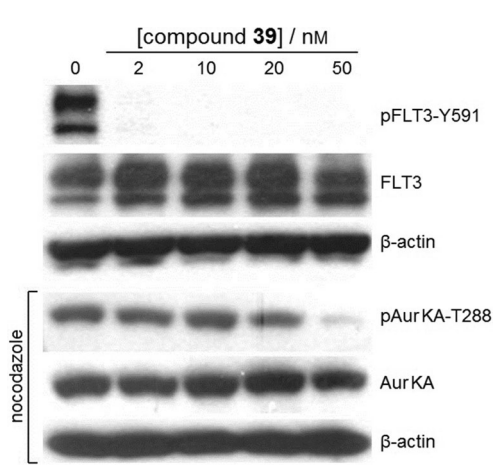

Figure 4. Western blotting analysis for cellular target modulation by compound **39**. Compound **39** inhibited phospho-FLT3 (Tyr591) and phospho-Aurora kinase A (Thr288) formation in MV4-11 at concentrations of <2 and ~50 nM, respectively.

Synthesis

Pyrimidine chlorides **40a–e** were prepared according to published procedures.[23,27–29] The pyrimidine chlorides were first treated with the commercially available thiazole side chain **41** via nucleophilic aromatic substitution, followed by deprotection with trifluoroacetic acid to produce the corresponding amine intermediates **42a–e** (Scheme 3). Urea formation of **42a–e** with isocyanates was carried out to afford urea compounds **27** and **33–37** in 17–28% overall yields. In addition, phenyl carbamates **43a** and **b** were synthesized following the procedure reported by Keith et al.[30] and further reacted with **42d** under basic condition in 1,4-dioxane to generate **38** and **39** in 74–81% yield (Scheme 4).

Conclusions

Computer-guided drug design has been used in conjunction with chemical synthesis and in vitro testing to identify dual FLT3–Aurora A inhibitors. The first screening yielded compound **27**, which exhibited FLT3 and Aurora kinase A inhibitory activity, with IC_{50} values of 322 and 43 nM, respectively. This discovery necessitated the chemical synthesis of just 26 compounds, emphasizing the highly efficient nature of in silico drug design. Structure–activity relationship studies and binding energy analysis of compound **27** and its analogues from Table 2 were conducted. The bioactivity data of these analogues was found to be highly consistent with the results of computer simulation, validating our use of binding energy calculations as a reliable strategy for the development of improved inhibitors.

In the second screening, both **38** and **39** were found to have the most promising dual kinase activities and were subjected to cellular activity tests. Dramatic antiproliferative effects of **39** against MOLM-13 and MV4-11 were observed, and its dual FLT3–Aurora A inhibitory mechanism was confirmed by

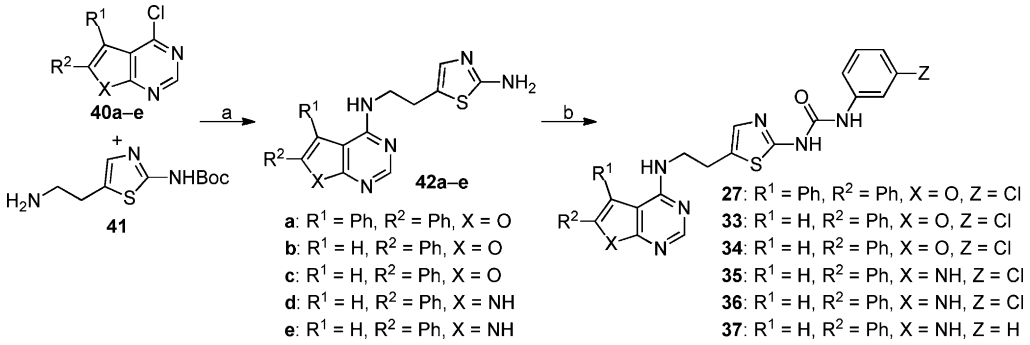

Scheme 3. *Reagents and conditions*: a) 1. Et_3N, EtOH or *tert*-BuOH, reflux, 15–24 h, 2. CF_3CO_2H, CH_2Cl_2, RT, 2 h, 42–59% over two steps; b) 3-Cl-PhNCO, or PhNCO, MeOH, CH_2Cl_2, RT, 16 h, 41–66%.

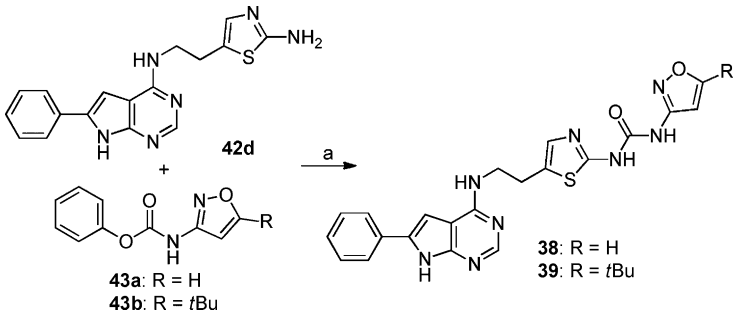

Scheme 4. *Reagents and conditions*: a) Et_3N, 1,4-dioxanes, reflux, 5 h, 74–81%.

Western blotting analysis. To summarize, we selected Aurora hit **5** as a starting point, followed by two consecutive computer-guided strategies, to rapidly and efficiently modify the side chain and the core to identify compound **39** as a potential anti-AML candidate for further development.

Experimental Section

Chemistry

General methods: All commercial chemicals and solvents were of reagent grade and used without further purification unless otherwise stated. All reactions were carried out under an atmosphere of dry nitrogen and were monitored by TLC, using Merck 60 F_{254} silica gel glass-backed plates (5×10 cm); zones were detected visually under UV irradiation (254 nm) or by spraying with phosphomolybdic acid reagent (Aldrich), followed by heating at 80 °C. Flash column chromatography was carried out using silica gel (Merck Kieselgel 60, no. 9385, 230–400 mesh ASTM). ^{1}H and ^{13}C NMR spectra were obtained with a Varian Mercury 300 or Varian Mercury 400 spectrometer, and the chemical shifts (δ) were recorded in ppm and reported relative to TMS or the solvent peak. High-resolution mass spectra (HRMS) were measured with a Finnigan (MAT-95XL) electron impact (EI) or by using Finnigan/Thermo Quest MAT 95XL FAB mass spectrometer. Low-resolution mass spectra (LRMS) data were measured on an Agilent MSD-1100 ESI-MS–MS system. Purity of the final compounds was determined with an Hitachi 2000 series HPLC system using a C_{18} column (Agilent ZORBAX Eclipse XDB-C18 5 μm, 4.6 mm×150 mm), operating at 25 °C. Elution was carried out using CH_3CN as mobile phase A and water containing 0.1% formic acid + 10 mmol NH_4OAc as mobile phase B. Elution conditions: 0 min, 10% phase A + 90% phase B; at 45 min, 90% phase A + 10% phase B; at 50 min, 10% phase A + 90% phase B; at 60 min, 10% phase A + 90% phase B. The flow rate of the mobile phase was 0.5 mL min^{-1}, and the injection volume of the sample was 5 μL. Peaks were detected at 210 nm. Purity of all the tested compounds were found to be >95% unless otherwise stated.

1-(3-Chlorophenyl)-3-(5-(2-(5,6-diphenylfuro[2,3-*d*]pyrimidin-4-ylamino)ethyl)thiazol-2-yl)urea (27): A solution containing **40a**[23] (92 mg, 0.30 mmol, 1.0 equiv), *tert*-butyl 5-(2-aminoethyl)thiazol-2-ylcarbamate (**41**, 109 mg, 0.448 mmol, 1.5 equiv), and triethylamine (61 mg, 0.60 mmol, 2.0 equiv) in EtOH (3.0 mL) was heated at reflux for 15 h. After the solvent was evaporated, the residue in CH_2Cl_2 (10.0 mL) was treated with trifluoroacetic acid (4.0 mL), and the mixture was stirred at room temperature for 2 h. The reaction mixture was concentrated under reduced pressure, and the residue was purified using gravity column chromatography on silica gel ($MeOH/CH_2Cl_2/NH_4OH$, 1:30:0.1 as the eluent) to give **42a** (68 mg, 0.16 mmol) in 53% yield as a white solid. 3-Chlorophenyl isocyanate (126 mg, 0.820 mmol, 5.1 equiv) was added to a solution of **42a** (68 mg, 0.16 mmol, 1.0 equiv) in a mixture of MeOH (1.0 mL) and CH_2Cl_2 (7.0 mL). The mixture was stirred at room temperature for 16 h. The reaction mixture was then concentrated under reduced pressure, and the residue was purified using gravity column chromatography on silica gel ($MeOH/CH_2Cl_2$=1:30 as the eluent) to give **27** (45 mg, 0.079 mmol) in 49% yield as a white solid: ^{1}H NMR (400 MHz, $CD_3OD + CDCl_3$): δ=2.96 (t, J=6.0 Hz, 2H), 3.71 (t, J=6.0 Hz, 2H), 6.89 (s, 1H), 7.03–7.06 (m,1H), 7.24–7.49 (m, 12H), 7.68 (t, J=2.0 Hz, 1H), 8.33 ppm (s, 1H); LC–MS (ESI) m/z 567 $[M+H]^+$.

1-(3-Chlorophenyl)-3-(5-(2-(6-phenylfuro[2,3-*d*]pyrimidin-4-ylamino)ethyl)thiazol-2-yl)urea (33): A solution containing **40b**[27] (69 mg, 0.30 mmol, 1.0 equiv), *tert*-butyl 5-(2-aminoethyl)thiazol-2-ylcarbamate (**41**, 109 mg, 0.448 mmol, 1.5 equiv), and triethylamine (61 mg, 0.60 mmol, 2.0 equiv) in EtOH (3.0 mL) was heated at reflux for 15 h. After the solvent was evaporated, the residue in CH_2Cl_2 (10 mL) was treated with trifluoroacetic acid (4.0 mL), and the mixture was stirred at room temperature for 2 h. The reaction mixture was concentrated under reduced pressure, and the residue was purified using gravity column chromatography on silica gel ($MeOH/CH_2Cl_2/NH_4OH$, 1:30:0.1, as the eluent) to give **42b** (45 mg, 0.13 mmol) in 44% yield as a white solid. 3-Chlorophenyl isocyanate (126 mg, 0.820 mmol, 6.3 equiv) was added to a solution of

42b (45 mg, 0.13 mmol, 1.0 equiv) in a mixture of MeOH (1.0 mL) and CH_2Cl_2 (7.0 mL). The mixture was stirred at room temperature for 16 h. The reaction mixture was then concentrated under reduced pressure and purified using gravity column chromatography on silica gel ($MeOH/CH_2Cl_2/NH_4OH$, 1:30:0.1, as the eluent) to give **33** (33 mg, 0.066 mmol) in 51% yield as a white solid: ^1H NMR (300 MHz, $[D_6]DMSO$): $\delta = 3.06$ (t, $J = 6.5$ Hz, 2H), 3.68–3.80 (m, 2H), 7.02–7.10 (m, 1H), 7.15 (s, 1H), 7.27–7.59 (m, 6H), 7.70 (s, 1H), 7.80 (d, $J = 7.7$ Hz, 2H), 8.19 (bs, 1H, NH), 8.29 (s, 1H), 9.16 ppm (s, 1H, NH); LC–MS (ESI) m/z 491 $[M+H]^+$; HPLC purity, 94.7%.

1-(3-Chlorophenyl)-3-(5-(2-(5-phenylfuro[2,3-*d*]pyrimidin-4-yl-amino)ethyl)thiazol-2-yl)urea (34): A solution containing **40c**[27] (52 mg, 0.23 mmol, 1.0 equiv), *tert*-butyl 5-(2-aminoethyl)thiazol-2-ylcarbamate (**41**, 109 mg, 0.448 mmol, 1.9 equiv), and triethylamine (67 mg, 0.66 mmol, 2.9 equiv) in EtOH (2.0 mL) was heated at reflux for 15 h. After the solvent was evaporated, the residue in CH_2Cl_2 (7.5 mL) was treated with trifluoroacetic acid (3.0 mL), and the mixture was stirred at room temperature for 2 h. The reaction mixture was concentrated under reduced pressure, and the residue was purified using gravity column chromatography on silica gel ($MeOH/CH_2Cl_2$, 1:20, as the eluent) to give **42c** (34 mg, 0.10 mmol) in 43% yield as a yellow solid. 3-Chlorophenyl isocyanate (126 mg, 0.820 mmol, 8.2 equiv) was added to a solution of **42c** (34 mg, 0.10 mmol, 1.0 equiv) in a mixture of MeOH (1.0 mL) and CH_2Cl_2 (7.0 mL). The mixture was stirred at room temperature for 16 h. The reaction mixture was then concentrated under reduced pressure and purified using gravity column chromatography on silica gel ($MeOH/CH_2Cl_2$, 1:20, as the eluent) to give **34** (32 mg, 0.066 mmol) in 66% yield as a white solid: ^1H NMR (300 MHz, CD_3OD): $\delta = 3.06$ (t, $J = 6.0$ Hz, 2H), 3.80 (t, $J = 6.0$ Hz, 2H), 6.99 (s, 1H), 7.06 (d, $J = 7.5$ Hz, 1H), 7.25–7.44 (m, 7H), 7.68–7.69 (m, 2H), 8.35 ppm (s, 1H); LC–MS (ESI) m/z 491 $[M+H]^+$.

1-(3-Chlorophenyl)-3-(5-(2-(6-phenyl-7*H*-pyrrolo[2,3-*d*]pyrimidin-4-ylamino)ethyl)thiazol-2-yl)urea (35): A solution containing **40d**[28] (45 mg, 0.24 mmol, 1.0 equiv) and *tert*-butyl 5-(2-aminoethyl)thiazol-2-ylcarbamate (**41**, 192 mg, 0.790 mmol, 3.3 equiv) in *tert*-butanol (2.0 mL) was heated at reflux for 24 h. After the solvent was evaporated, the residue in CH_2Cl_2 (4.0 mL) was treated with trifluoroacetic acid (2.0 mL), and the mixture was stirred at room temperature for 4 h. The reaction mixture was concentrated under reduced pressure, and the residue was purified using gravity column chromatography on silica gel ($MeOH/CH_2Cl_2/NH_4OH$, 1:9:0.1, as the eluent) to give **42d** (34 mg, 0.10 mmol) in 42% yield as a yellow solid: ^1H NMR (300 MHz, $[D_6]DMSO$): $\delta = 2.90$ (t, $J = 6.8$ Hz, 2H), 3.61 (td, $J = 6.8$, 5.1 Hz, 2H), 6.65 (s, 2H), 6.68 (s, 1H), 6.93 (s, 1H), 7.27 (t, $J = 7.7$ Hz, 1H), 7.42 (t, $J = 7.7$ Hz, 2H), 7.59 (t, $J = 5.1$ Hz, 1H), 7.76 (d, $J = 7.7$ Hz, 2H), 8.12 (s, 1H), 12.02 ppm (bs, 1H); LC–MS (ESI) m/z 337 $[M+H]^+$. 3-Chlorophenyl isocyanate (126 mg, 0.820 mmol, 8.2 equiv) was added to a solution of **42d** (34 mg, 0.10 mmol, 1.0 equiv) in a mixture of MeOH (1.0 mL) and CH_2Cl_2 (7.0 mL). The mixture was stirred at room temperature for 16 h. The reaction mixture was then concentrated under reduced pressure and purified using gravity column chromatography on silica gel ($MeOH/CH_2Cl_2/NH_4OH$, 1:9:0.1, as the eluent) to give **35** (20 mg, 0.041 mmol) in 41% yield as a white solid: ^1H NMR (400 MHz, $[D_6]DMSO$): $\delta = 2.99$–3.07 (m, 2H), 3.56–3.74 (m, 2H), 6.92 (s, 1H), 7.00–7.07 (m, 1H), 7.12 (s, 1H), 7.25–7.33 (m, 3H), 7.42 (t, $J = 7.7$ Hz, 2H), 7.62–7.71 (m, 2H), 7.77 (d, $J = 7.7$ Hz, 2H), 8.14 (s, 1H), 9.13 (bs, 1H), 10.44 (bs, 1H), 12.05 ppm (bs, 1H); LC–MS (ESI) m/z 490 $[M+H]^+$.

1-(3-Chlorophenyl)-3-(5-(2-(5-phenyl-7*H*-pyrrolo[2,3-*d*]pyrimidin-4-ylamino)ethyl)thiazol-2-yl)urea (36): A solution containing **40e**[29] (24 mg, 0.10 mmol, 1.0 equiv) and *tert*-butyl 5-(2-aminoethyl)thiazol-2-ylcarbamate (**41**, 80 mg, 0.33 mmol, 3.3 equiv) in *tert*-butanol (1.0 mL) was heated at reflux for 24 h. After the solvent was evaporated, the residue in CH_2Cl_2 (2.0 mL) was treated with trifluoroacetic acid (1.0 mL), and the mixture was stirred at room temperature for 4 h. The reaction mixture was concentrated under reduced pressure, and the residue was purified using gravity column chromatography on silica gel ($MeOH/CH_2Cl_2/NH_4OH$, 1:9:0.1, as the eluent) to give **42e** (20 mg, 0.059 mmol) in 59% yield as a yellow solid. 3-Chlorophenyl isocyanate (70 mg, 0.46 mmol, 7.7 equiv) was added to a solution of **42e** (20 mg, 0.059 mmol, 1.0 equiv) in a mixture of MeOH (0.50 mL) and CH_2Cl_2 (3.5 mL). The mixture was stirred at room temperature for 16 h. The reaction mixture was then concentrated under reduced pressure and purified using gravity column chromatography on silica gel ($MeOH/CH_2Cl_2/NH_4OH$, 1:9:0.1, as the eluent) to give **36** (13 mg, 0.027 mmol) in 45% yield as a white solid: ^1H NMR (400 MHz, CD_3OD): $\delta = 3.02$ (t, $J = 6.0$ Hz, 2H), 3.75 (t, $J = 6.0$ Hz, 2H), 6.89 (s, 1H), 7.01–7.04 (m,1H), 7.07 (s, 1H), 7.24–7.38 (m, 7H), 7.67 (t, $J = 2.0$ Hz, 1H), 8.20 ppm (s, 1H); LC–MS (ESI) m/z 490 $[M+H]^+$.

1-Phenyl-3-(5-(2-(6-phenyl-7*H*-pyrrolo[2,3-*d*]pyrimidin-4-yl-amino)ethyl)thiazol-2-yl)urea (37): Phenyl isocyanate (178 mg, 1.49 mmol, 8.3 equiv) was added to a solution of **42d** (60 mg, 0.18 mmol, 1.0 equiv) in a mixture of MeOH (1.5 mL) and CH_2Cl_2 (10 mL). The mixture was stirred at room temperature for 16 h. The reaction mixture was then concentrated under reduced pressure and purified using gravity column chromatography on silica gel ($MeOH/CH_2Cl_2/NH_4OH$, 1:9:0.1, as the eluent) to give **37** (40 mg, 0.088 mmol) in 49% yield as a white solid: ^1H NMR (400 MHz, $[D_6]DMSO$): $\delta = 3.04$ (t, $J = 6.2$ Hz, 2H), 3.65–3.75 (m, 2H), 6.93 (s, 1H), 7.00 (t, $J = 7.2$ Hz, 1H), 7.12 (s, 1H), 7.24–7.32 (m, 3H), 7.39–7.47 (m, 4H), 7.64 (bs, 1H), 7.77 (d, $J = 7.7$ Hz, 2H), 8.14 (s, 1H), 8.92 (bs, 1H), 10.29 (bs, 1H), 12.04 ppm (bs, 1H); LC–MS (ESI) m/z 456 $[M+H]^+$.

1-(1,2-Oxazol-3-yl)-3-(5-{2-[(6-phenyl-7*H*-pyrrolo[2,3-*d*]pyrimidin-4-yl)amino]ethyl}-1,3-thiazol-2-yl)urea (38): A solution containing **42d** (50 mg, 0.15 mmol, 1.0 equiv), phenyl 1,2-oxazol-3-ylcarbamate[30] (**43a**, 50 mg, 0.24 mmol, 1.6 equiv), and triethylamine (45 mg, 0.44 mmol, 3.0 equiv) in 1,4-dioxane (3.5 mL) was heated at reflux for 5 h. The reaction mixture was concentrated under reduced pressure, and the residue was purified using gravity column chromatography on silica gel ($MeOH/CH_2Cl_2/NH_4OH$, 1:9:0.1, as the eluent) to give **38** (54 mg, 0.12 mmol) in 81% yield as a white solid: ^1H NMR (400 MHz, $[D_6]DMSO$): $\delta = 3.02$–3.09 (m, 2H), 3.64–3.74 (m, 2H), 6.84 (d, $J = 1.2$ Hz, 1H), 6.92 (d, $J = 1.8$ Hz, 1H), 7.15 (s, 1H), 7.27 (t, $J = 7.4$ Hz, 1H), 7.42 (dd, $J = 7.5$, 7.4 Hz, 2H), 7.64 (t, $J = 5.4$ Hz, 1H), 7.77 (d, $J = 7.5$ Hz, 2H), 8.14 (s, 1H), 8.75 (d, $J = 1.2$ Hz, 1H), 9.84 (bs, 1H), 10.41 (bs, 1H), 12.04 ppm (bs, 1H); LC–MS (ESI) m/z 447 $[M+H]^+$.

1-(5-*tert*-Butyl-1,2-oxazol-3-yl)-3-(5-{2-[(6-phenyl-7*H*-pyrrolo[2,3-*d*]pyrimidin-4-yl)amino]ethyl}-1,3-thiazol-2-yl)urea (39): A solution containing **42d** (50 mg, 0.15 mmol, 1.0 equiv), phenyl (5-*tert*-butylisoxazol-3-yl)carbamate[30] (**43b**, 70 mg, 0.27 mmol, 1.8 equiv), and triethylamine (45 mg, 0.44 mmol, 3.0 equiv) in 1,4-dioxane (3.5 mL) was heated at reflux for 5 h. The reaction mixture was concentrated under reduced pressure, and the residue was purified using gravity column chromatography on silica gel ($MeOH/CH_2Cl_2/NH_4OH$, 1:9:0.1, as the eluent) to give **39** (56 mg, 0.11 mmol) in 74% yield as a white solid: ^1H NMR (400 MHz, $[D_6]DMSO$): $\delta = 1.26$ (s, 9H), 3.02–3.09 (m, 2H), 3.64–3.75 (m, 2H), 6.50 (s, 1H), 6.92 (s, 1H), 7.15 (s, 1H), 7.27 (t, $J = 7.1$ Hz, 1H), 7.42 (dd, $J = 7.7$, 7.1 Hz, 2H), 7.63 (bs, 1H), 7.77 (d, $J = 7.7$ Hz, 2H), 8.14 (s, 1H), 9.73 (bs,

1H), 10.37 (bs, 1H), 12.04 ppm (bs, 1H); LC–MS (ESI) *m/z* 447 $[M+H]^+$.

Biological methods

FLT3 kinase assay: FLT3 assays were conducted as previously described.[31] GST-FLT3-KD^{WT} containing the FLT3 kinase catalytic domain (residues Tyr567–Ser993) were expressed in Sf9 insect cells transfected with the baculovirus containing pBac-PAK8-GST-FLT3-KD plasmid. FLT3^{WT} Kinase-Glo assays were carried out in 96-well plates at 30 °C for 4 h with tested compounds at a final volume of 50 μL including the following components: 75 ng GST-FLT3-KD^{WT} proteins, 25 mM HEPES, pH 7.4, 4 mM $MnCl_2$, 10 mM $MgCl_2$, 2 mM DTT, 0.02% Triton X-100, 0.1 mg mL^{-1} bovine serum albumin, 25 μM Her2 peptide substrate, 0.5 mM Na_3VO_4, and 1 μM ATP.

Aurora kinase A assay: Aurora kinase A assays were conducted as previously described.[27] The recombinant GST-Aurora kinase A (residues Ser123–Ser401) containing the kinase domain was expressed in Sf9 insect cells. The kinase assay was carried out in 96-well plates with tested compound in a final volume of 50 μL at 37 °C for 90 min with the following components: 50 mM Tris-HCl pH 7.4, 10 mM NaCl, 10 mM $MgCl_2$, 0.01% BSA, 5 μM ATP, 1 mM DTT, 15 μM tetra(-LRRASLG) peptide, and 150 ng recombinant Aurora kinase A.

Following incubation, 50 μL Kinase-Glo Plus Reagent (Promega, Madison, WI, USA) was added, and the mixture was incubated at 25 °C for 20 min. A 70 μL aliquot of each reaction mixture was transferred to a black microliter plate, and luminescence was measured on a Wallac Vector 1420 multilabel counter (PerkinElmer, Shelton, CT, USA).

Cell lines and MTS cell viability assay: The MTS cell viability assay was conducted as previously described.[31] The MOLM-13 human leukemia cell line was obtained from the German Resource Centre for Biological Material (DSMZ, Braunschweig, Germany); the MV4-11 cell line was purchased from the American Type Culture Collection (ATCC, Manassas, VA, USA). All leukemia cell lines were maintained in RPMI 1640 medium supplemented with 10% fetal bovine serum (FBS), 10 U mL^{-1} penicillin, and 10 g mL^{-1} streptomycin at 37 °C and 5% CO_2. To determine cell viability after drug treatment, assays were performed by seeding 10000 cells (leukemia cell lines) per well in a 96-well culture plate. After 16 h, cells were then treated with vehicle or various concentrations of compound in medium for 72 h. Viable cells were quantitated using the MTS method (Promega, Madison, WI, USA) according to the manufacturer's recommended protocol. Results were determined by measuring the absorbance at 490 nm using a plate reader (Victor2; PerkinElmer, Shelton, CT, USA). The IC_{50} value was defined as the amount of compound that caused a 50% reduction in cell viability in comparison with DMSO-treated (vehicle) control and was calculated using Prism version 4 software (GraphPad, San Diego, CA, USA).

Western blotting analysis: Western blot analysis was conducted as previously described.[32,33] Primary antibodies against phospho-FLT3 (Tyr591) and phospho-Aurora kinase A (Thr288) were purchased from Cell Signaling Technology. The anti-FLT3 antibody and anti-Aurora kinase A antibody were purchased from Santa Cruz Biotechnology and Upstate, respectively. The anti-β-actin monoclonal antibody was purchased from GeneTex. The secondary antibodies horseradish peroxidase (HRP)-linked goat anti-rabbit IgG were purchased from Jackson Immuno. MV4-11 cells were incubated with compound **39** for 2 h at the indicated concentrations. Cell lysates were prepared and analyzed by immunoblotting. For Aurora kinase A analysis, the cell lysates were obtained from MV4-11 cells incubated for 16 h with 50 ng mL^{-1} nocodazole, followed by drug treatment for 2 h at the indicated concentrations.

Acknowledgements

Financial support from the Taiwanese National Health Research Institutes and the National Science Council, Taiwan (NSC-101-2113-M-400-002-MY4 and NSC-102-2325-B-400-003 to H.-P.H., NSC 102-2113-M-400-003-MY3 to H.-Y.S.) is gratefully acknowledged. Y.C.H. is supported by a postdoctoral fellowship from the National Science Council, Taiwan.

Keywords: Aurora kinase A · drug design · FLT3 · inhibitors · leukemia

[1] M. E. M. Noble, J. A. Endicott, L. N. Johnson, *Science* **2004**, *303*, 1800–1805.
[2] J. M. Goldman, J. V. Melo, *N. Engl. J. Med.* **2003**, *349*, 1451–1464.
[3] P. Cohen, D. R. Alessi, *ACS Chem. Biol.* **2013**, *8*, 96–104.
[4] US Food and Drug Administration (FDA), *Drugs@FDA*, FDA-Approved Drug Products: http://www.accessdata.fda.gov/scripts/cder/drugsatfda/index.cfm.
[5] G. Manning, D. B. Whyte, R. Martinez, T. Hunter, S. Sudarsanam, *Science* **2002**, *298*, 1912–1934.
[6] A. Markovic, K. L. MacKenzie, R. B. Lock, *Int. J. Biochem. Cell Biol.* **2005**, *37*, 1168–1172.
[7] D. G. Gilliland, J. D. Griffin, *Blood* **2002**, *100*, 1532–1542.
[8] B. W. Parcells, A. K. Ikeda, T. Simms-Waldrip, T. B. Moore, K. M. Sakamoto, *Stem Cells* **2006**, *24*, 1174–1184.
[9] S. H. Chu, D. Small, *Drug Resist. Updates* **2009**, *12*, 8–16.
[10] T. Kindler, D. B. Lipka, T. Fischer, *Blood* **2010**, *116*, 5089–5102.
[11] D. W. Sternberg, J. D. Licht, *Curr. Opin. Hematol.* **2005**, *12*, 7–13.
[12] C. H. A. Cheung, M. S. Coumar, H.-P. Hsieh, J.-Y. Chang, *Expert Opin. Invest. Drugs* **2009**, *18*, 379–398.
[13] A. A. Mortlock, K. M. Foote, N. M. Heron, F. H. Jung, G. Pasquet, J.-J. M. Lohmann, N. Warin, F. Renaud, C. De Savi, N. J. Roberts, T. Johnson, C. B. Dousson, G. B. Hill, D. Perkins, G. Hatter, R. W. Wilkinson, S. R. Wedge, S. P. Heaton, R. Odedra, N. J. Keen, C. Crafter, E. Brown, K. Thompson, S. Brightwell, L. Khatri, M. C. Brady, S. Kearney, D. McKillop, S. Rhead, T. Parry, S. Green, *J. Med. Chem.* **2007**, *50*, 2213–2224.
[14] A. S. Moore, A. Faisal, D. Gonzalez de Castro, V. Bavetsias, C. Sun, B. Atrash, M. Valenti, A. de Haven Brandon, S. Avery, D. Mair, F. Mirabella, J. Swansbury, A. D. J. Pearson, P. Workman, J. Blagg, F. I. Raynaud, S. A. Eccles, S. Linardopoulos, *Leukemia* **2012**, *26*, 1462–1470.
[15] V. Bavetsias, S. Crumpler, C. Sun, S. Avery, B. Atrash, A. Faisal, A. S. Moore, M. Kosmopoulou, N. Brown, P. W. Sheldrake, K. Bush, A. Henley, G. Box, M. Valenti, A. d. H. Brandon, F. I. Raynaud, P. Workman, S. A. Eccles, R. Bayliss, S. Linardopoulos, J. Blagg, *J. Med. Chem.* **2012**, *55*, 8721–8734.
[16] P. P. Zarrinkar, R. N. Gunawardane, M. D. Cramer, M. F. Gardner, D. Brigham, B. Belli, M. W. Karaman, K. W. Pratz, G. Pallares, Q. Chao, K. G. Sprankle, H. K. Patel, M. Levis, R. C. Armstrong, J. James, S. S. Bhagwat, *Blood* **2009**, *114*, 2984–2992.
[17] D. M. Goldstein, N. S. Gray, P. P. Zarrinkar, *Nat. Rev. Drug Discovery* **2008**, *7*, 391–397.
[18] F. Ciardiello, G. Tortora, *N. Engl. J. Med.* **2008**, *358*, 1160–1174.
[19] H. A. Burris III, *Oncologist* **2004**, *9*, 10–15.
[20] M. S. Coumar, C.-Y. Chu, C.-W. Lin, H.-Y. Shiao, Y.-L. Ho, R. Reddy, W.-H. Lin, C.-H. Chen, Y.-H. Peng, J.-S. Leou, T.-W. Lien, C.-T. Huang, M.-Y. Fang, S.-H. Wu, J.-S. Wu, S. K. Chittimalla, J.-S. Song, J. T.-A. Hsu, S.-Y. Wu, C.-C. Liao, Y.-S. Chao, H.-P. Hsieh, *J. Med. Chem.* **2010**, *53*, 4980–4988.
[21] Y.-H. Peng, H.-Y. Shiao, C.-H. Tu, P.-M. Liu, J. T.-A. Hsu, P. K. Amancha, J.-S. Wu, M. S. Coumar, C.-H. Chen, S.-Y. Wang, W.-H. Lin, H.-Y. Sun, Y.-S. Chao, P.-C. Lyu, H.-P. Hsieh, S.-Y. Wu, *J. Med. Chem.* **2013**, *56*, 3889–3903.

[22] The details of the homology modeling structure will be published separately.
[23] M. S. Coumar, M.-T. Tsai, C.-Y. Chu, B.-J. Uang, W.-H. Lin, C.-Y. Chang, T.-Y. Chang, J.-S. Leou, C.-H. Teng, J.-S. Wu, M.-Y. Fang, C.-H. Chen, J. T.-A. Hsu, S.-Y. Wu, Y.-S. Chao, H.-P. Hsieh, *ChemMedChem* **2010**, *5*, 255 – 267.
[24] J.-M. Wu, C.-T. Chen, M. S. Coumar, W.-H. Lin, Z.-J. Chen, J. T.-A. Hsu, Y.-H. Peng, H.-Y. Shiao, W.-H. Lin, C.-Y. Chu, J.-S. Wu, C.-T. Lin, C.-P. Chen, C.-C. Hsueh, K.-Y. Chang, L.-P. Kao, C.-Y. F. Huang, Y.-S. Chao, S.-Y. Wu, H.-P. Hsieh, Y.-H. Chi, *Proc. Natl. Acad. Sci. USA* **2013**, *110*, E1779 – E1787.
[25] D. Fancelli, J. Moll, M. Varasi, R. Bravo, R. Artico, D. Berta, S. Bindi, A. Cameron, I. Candiani, P. Cappella, P. Carpinelli, W. Croci, B. Forte, M. L. Giorgini, J. Klapwijk, A. Marsiglio, E. Pesenti, M. Rocchetti, F. Roletto, D. Severino, C. Soncini, P. Storici, R. Tonani, P. Zugnoni, P. Vianello, *J. Med. Chem.* **2006**, *49*, 7247 – 7251.
[26] Y.-Y. Ke, H.-Y. Shiao, Y. C. Hsu, C.-Y. Chu, W.-C. Wang, Y.-C. Lee, W.-H. Lin, C.-H. Chen, J. T. A. Hsu, C.-W. Chang, C.-W. Lin, T.-K. Yeh, Y.-S. Chao, M. S. Coumar, H.-P. Hsieh, *ChemMedChem* **2013**, *8*, 136 – 148.
[27] H.-Y. Shiao, M. S. Coumar, C.-W. Chang, Y.-Y. Ke, Y.-H. Chi, C.-Y. Chu, H.-Y. Sun, C.-H. Chen, W.-H. Lin, K.-S. Fung, P.-C. Kuo, C.-T. Huang, K.-Y. Chang, C.-T. Lu, J. T.-A. Hsu, C.-T. Chen, W.-T. Jiaang, Y.-S. Chao, H.-P. Hsieh, *J. Med. Chem.* **2013**, *56*, 5247 – 5260.
[28] S. J. Kaspersen, C. Sørum, V. Willassen, E. Fuglseth, E. Kjøbli, G. Bjørkøy, E. Sundby, B. H. Hoff, *Eur. J. Med. Chem.* **2011**, *46*, 6002 – 6014.
[29] B. C. Bookser, B. G. Ugarkar, M. C. Matelich, R. H. Lemus, M. Allan, M. Tsuchiya, M. Nakane, A. Nagahisa, J. B. Wiesner, M. D. Erion, *J. Med. Chem.* **2005**, *48*, 7808 – 7820.
[30] J. M. Keith, R. Apodaca, W. Xiao, M. Seierstad, K. Pattabiraman, J. Wu, M. Webb, M. J. Karbarz, S. Brown, S. Wilson, B. Scott, C.-S. Tham, L. Luo, J. Palmer, M. Wennerholm, S. Chaplan, J. G. Breitenbucher, *Bioorg. Med. Chem. Lett.* **2008**, *18*, 4838 – 4843.
[31] W.-H. Lin, S.-Y. Hsieh, S.-C. Yen, C.-T. Chen, T.-K. Yeh, T. Hsu, C.-T. Lu, C.-P. Chen, C.-W. Chen, L.-H. Chou, Y.-L. Huang, A.-H. Cheng, Y.-I. Chang, Y.-J. Tseng, K.-R. Yen, Y.-S. Chao, J. T.-A. Hsu, W.-T. Jiaang, *Bioorg. Med. Chem.* **2011**, *19*, 4173 – 4182.
[32] J. T.-A. Hsu, T.-K. Yeh, S.-C. Yen, C.-T. Chen, S.-Y. Hsieh, T. Hsu, C.-T. Lu, C.-W. Chen, L.-H. Chou, C.-H. Chiu, Y.-I. Chang, Y.-J. Tseng, K.-R. Yen, Y.-S. Chao, W.-H. Lin, W.-T. Jiaang, *Bioorg. Med. Chem. Lett.* **2012**, *22*, 4654 – 4659.
[33] M. S. Coumar, J.-S. Leou, P. Shukla, J.-S. Wu, A. K. Dixit, W.-H. Lin, C.-Y. Chang, T.-W. Lien, U.-K. Tan, C.-H. Chen, J. T.-A. Hsu, Y.-S. Chao, S.-Y. Wu, H.-P. Hsieh, *J. Med. Chem.* **2009**, *52*, 1050 – 1062.

Received: December 30, 2013
Published online on ■■ ■■, 0000

Y. Chang Hsu, Y.-Y. Ke, H.-Y. Shiao, C.-C. Lee, W.-H. Lin, C.-H. Chen, K.-J. Yen, J. T.-A. Hsu, C. Chang, H.-P. Hsieh**

■■ – ■■

Facile Identification of Dual FLT3–Aurora A Inhibitors: A Computer-Guided Drug Design Approach

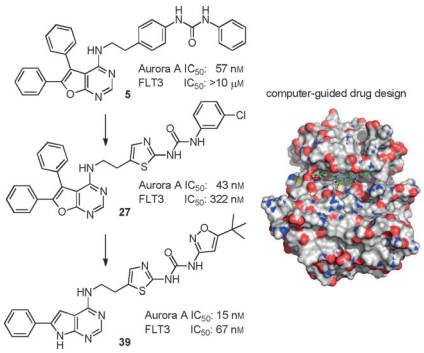

In silico selection: We selected an Aurora hit compound as a starting point, followed by two consecutive computer-guided strategies to rapidly and efficiently modify the side chain and core. These efforts resulted in the identification of a potential FLT3–Aurora A inhibitor for further development to treat acute myeloid leukemia (AML).